XLVI CILAMCE
VITÓRIA - ES - BRAZIL - 2025
XLVI IBERO-LATIN AMERICAN CONGRESS ON COMPUTATIONAL METHODS IN ENGENEERING

Improving Convergence and Robustness of the Phase-Field Method for Fracture Modeling using a Gradient-based Line Search Strategy for the L-BFGS Algorithm

Caio S. Ramos[1], Carlos A. Duarte[2], Nathan Shauer[3], Sergio P.B. Proença[1]

[1]*Department of Structural Engineering, Sao Carlos School of Engineering, University of Sao Paulo*
400 Trabalhador Sao Carlense Avenue, Parque Arnold Schimidt, 13564-030, Sao Carlos, Sao Paulo, Brazil
caio_silva@usp.br, persival@sc.usp.br
[2]*Department of Civil and Environmental Engineering, University of Illinois at Urbana-Champaign, Newmark Laboratory*
205 North Mathews Avenue, Urbana, Illinois, USA
caduarte@illinois.edu
[3]*LabMeC-FECAU, State University of Campinas*
85 Josiah Willard Gibbs Street, Cidade Universitaria, Campinas, Sao Paulo, Brazil
shauer@unicamp.br

Abstract. Phase-field models are widely recognized for their capability to simulate intricate crack propagation processes. Despite their advantages, the nonlinear and non-convex nature of their variational formulation poses significant challenges for numerical solvers, particularly in scenarios involving rapid crack growth. Traditional Newton-based solvers often struggle with convergence, while the commonly used alternating minimization approach, though robust, leads to high computational costs due to its iterative nature. In this presentation, we introduce a novel improvement to the L-BFGS algorithm by incorporating a gradient-based line search strategy. This modification aims to improve both the efficiency and robustness of phase-field fracture simulations. We showcase numerical experiments involving brittle and quasi-brittle fracture cases, highlighting the method's ability to reduce computational costs while maintaining accuracy. A stand-alone implementation of the proposed method is provided, allowing for easy integration into existing phase-field frameworks.

Keywords: Phase-field, Fracture, Line search, L-BFGS, Staggered, Quasi-Newton

1 Introduction

The mechanics of damage and failure in engineering applications are essential for structural safety. An accurate assessment of crack propagation behavior can enhance the prediction of limit load capacity and optimize the dimensions of structural components. Griffith [1] proposed the first theory for brittle crack evolution, and since then, several numerical methods have been developed to model crack propagation in solids, classified into two categories: discrete crack approaches (where the crack is explicitly modeled as a discontinuity using re-meshing strategies or enriching the displacement field with discontinuous functions [2–4]) and continuous crack approaches (where the crack is implicitly modeled through a continuous field variable).

Phase-field models for fracture are energy-based frameworks [5, 6] that have gained popularity due to their ability to model complex crack configurations without needing ad hoc criteria or tracking algorithms. These models provide a variational formulation of Griffith-type fracture mechanics, describing the competition between elastic and fracture energy potentials. Sharp cracks are approximated as diffuse regions characterized by a phase-field variable, enabling a smooth transition between cracked and uncracked states of the material.

The formulation results in a non-convex and strongly nonlinear energy functional with respect to both displacement and phase-field variables. Standard Newton-Raphson-based monolithic solvers do not perform satisfactorily in this situation, typically diverging, especially during brutal crack evolution [7, 8]. To overcome this issue, several attempts have been made, including system energy-dependent line search [7], modified Newton methods [9], and inertial corrections [10]. However, the most employed technique consists of decoupling the weak formulation by alternately updating displacement and phase-field variables (alternating minimization algorithm - AM)

[11, 12], which is very robust but computationally demanding.

This work explores a quasi-Newton method of BFGS (Broyden-Fletcher-Goldfarb-Shanno) type in the context of phase-field models for fracture analysis. The BFGS approach has been claimed as a promising alternative due to its computational efficiency and robustness [13–15]. A modified version of BFGS is proposed for non-convex functionals, along with a new quasi-newton line search strategy to improve the robustness of monolithic approaches. Representative numerical examples involving mode I and mixed I+II are presented to demonstrate the performance of the proposed algorithm compared to the AM solver, covering both brittle and quasi-brittle fracture analyses.

2 Mathematical model

The mathematical model considers a linear elastic body $\bar{\Omega} = \Omega \cup \partial\Omega$ in $\mathbb{R}^d$ with external boundary $\partial\Omega$ and internal discontinuity boundaries $\Gamma \subset \mathbb{R}^{d-1}$, subjected to quasi-static loading at pseudo-time t_n. The system is kinematically described by displacement field $\boldsymbol{u}(\boldsymbol{x}, t_n)$ with prescribed displacements $\bar{\boldsymbol{u}}_n$ on boundary $\partial\Omega_u$. No body forces are considered.

Based on the variational approach of the Griffith's theory proposed by Francfort and Marigo [5], Bourdin et al. [6] introduced a regularization of the crack surface by adding a scalar phase-field $\phi(\boldsymbol{x})$ to the body's kinematics, yielding the regularized energy functional

$$\tilde{\mathcal{E}}(\boldsymbol{u}, \phi) = \int_\Omega \psi_s(\boldsymbol{\varepsilon}, \phi)\mathrm{d}\Omega + \mathcal{G}_c \int_\Omega \gamma(\phi, \nabla\phi)\mathrm{d}\Omega. \tag{1}$$

The crack surface density function $\gamma(\phi, \nabla\phi)$ approximates the sharp crack set Γ through a localized band $\Omega_\phi \subseteq \Omega$ where the damage field takes value 1 on cracks and smoothly decreases to 0 elsewhere. The degraded elastic strain energy is expressed as $\psi_s(\boldsymbol{\varepsilon}, \phi) = g(\phi)\psi_0(\boldsymbol{\varepsilon})$, where $g(\phi)$ is a continuous monotonically decreasing function satisfying boundary conditions $g(0) = 1$ (intact state), $g(1) = 0$ (completely broken state). For isotropic linear elasticity, the elastic strain energy density function is $\psi_0(\boldsymbol{\varepsilon}) = \frac{1}{2}\lambda \mathrm{tr}^2(\boldsymbol{\varepsilon}) + \mu \mathrm{tr}(\boldsymbol{\varepsilon}^2)$ with Lamé coefficients λ and μ. Considering small displacements and deformations, the infinitesimal strain tensor is defined as $\boldsymbol{\varepsilon}(\boldsymbol{u}) = \frac{1}{2}\left(\nabla\boldsymbol{u} + (\nabla\boldsymbol{u})^T\right)$, where $\nabla\boldsymbol{u}$ is the gradient of the displacement field $\boldsymbol{u}$, and $\mathcal{G}_c$ being the critical energy release rate.

The crack surface density function is formulated as

$$\gamma(\phi, \nabla\phi) = \frac{1}{c_w}\left(\frac{w(\phi)}{\ell} + \ell|\nabla\phi|^2\right), \tag{2}$$

where $w(\phi)$ is the local dissipated fracture energy density with properties $w(0) = 0$, $w(1) = 1$, and $w'(\phi) \geq 0$ for $\phi \in [0, 1]$. The length scale parameter ℓ governs the localization band size, and the normalization constant $c_w = \int_0^1 \sqrt{w(z)}\,\mathrm{d}z$ ensures Γ-convergence as $\ell \to 0$.

The functions $w(\phi)$ and $g(\phi)$ plays a central role to characterize the regularized potential energy described in (1). Herein, we consider the Ambrosio-Tortorelli (AT) family of functions [16] to define the stiffness degradation function $g(\phi)$ and the crack surface density function $w(\phi)$, especifically the `AT2` model, which is widely used in the literature [12, 17] and defined as $w(\phi) = \phi^2$, $g(\phi) = (1-\phi)^2$ and $c_w = 2$. This formulation results in an exponential damage distribution with infinite support and no linear elastic stage before peak strength.

2.1 Variational formulation

Following a variational approach, given a load step $n \geq 1$, the state of the system described by $(\boldsymbol{u}, \phi)$ is represented by the solution of the following minimization problem

$$\arg\min\{\tilde{\mathcal{E}}(\boldsymbol{u}, \phi) \mid \boldsymbol{u} \in \boldsymbol{\mathcal{V}}_n,\ \phi \in \mathcal{D}_n\}, \tag{3}$$

where the trial solution space for displacement and damage fields are $\boldsymbol{\mathcal{V}}_n := \left\{\boldsymbol{u} \in [H^1(\Omega)]^d \mid \boldsymbol{u} = \bar{\boldsymbol{u}}_n \text{ on } \partial\Omega_u\right\}$ and $\mathcal{D}_n := \left\{\phi \in H^1(\Omega) \mid \phi \in [0,\ 1],\ \phi \geq \phi_{n-1} \text{ in } \Omega\right\}$, respectively. Similarly, the test function space for displacement field is defined as $\boldsymbol{\mathcal{V}}_0 := \left\{\delta\boldsymbol{u} \in [H^1(\Omega)]^d \mid \delta\boldsymbol{u} = \boldsymbol{0} \text{ on } \partial\Omega_u\right\}$. An important aspect of phase-field damage models is ensuring that no crack healing occurs between loading steps, as is required by the irreversibility condition $\phi \geq \phi_{n-1}$. A widely adopted approach is to use a monotonic history field $\mathcal{H}(\boldsymbol{x}) := \max_{n\geq 1}\{\mathcal{H}_{n-1},\ \bar{\mathcal{H}}\}$ [11] to implicitly impose the irreversibility constraint, where $\bar{\mathcal{H}}$ is called *driving force*. However, such an approximation is no longer variationally consistent. Then, the first variation of the energy functional in (1) with respect to

$\boldsymbol{u}$ and ϕ, respectively, reads as follow

$$\begin{aligned}\tilde{\mathcal{E}}_{\boldsymbol{u}}(\boldsymbol{u},\phi;\delta\boldsymbol{u}) &= \int_\Omega g(\phi)\left(\frac{\partial\psi_0}{\partial\boldsymbol{\varepsilon}} : \frac{\partial\boldsymbol{\varepsilon}}{\partial\boldsymbol{u}}\delta\boldsymbol{u}\right)\,\mathrm{d}\Omega \\ \hat{\mathcal{E}}_{\phi}(\boldsymbol{u},\phi;\delta\phi) &= \int_\Omega g'(\phi)\mathcal{H}\delta\phi\,\mathrm{d}\Omega + \frac{\mathcal{G}_c}{c_w}\int_\Omega\left(\frac{w'(\phi)}{\ell}\delta\phi + 2\ell\nabla\phi\cdot\nabla\delta\phi\right)\mathrm{d}\Omega.\end{aligned} \tag{4}$$

The solution $(\boldsymbol{u},\phi)\in\boldsymbol{\mathcal{V}}_n\times\mathcal{D}_n$ at loading step $n\geq 1$ must satisfy the system of equations

$$\tilde{\mathcal{E}}_{\boldsymbol{u}}(\boldsymbol{u},\phi;\delta\boldsymbol{u})=0,\quad\forall\,\delta\boldsymbol{u}\in\boldsymbol{\mathcal{V}}_0,\quad\hat{\mathcal{E}}_{\phi}(\boldsymbol{u},\phi;\delta\phi)=0,\quad\forall\,\delta\phi\in\mathcal{D}_n. \tag{5}$$

The driving force variable, $\bar{\mathcal{H}}$, governs how the phase-field damage evolves. In this work, the hybrid phase-field model by Ambati et al. [18] is employed, where $\bar{\mathcal{H}}=\psi_0^+(\boldsymbol{\varepsilon})$ is employed following Miehe et al. [11], with $\psi_0^+(\boldsymbol{\varepsilon})$ is the positive part of the elastic potential energy.

3 Solution algorithms

The Newton-Raphson method starts with the solution $\mathbf{z}:=\{\boldsymbol{u}^h,\phi^h\}$ and residual vector $\mathbf{g}:=\{\mathbf{r}^{\boldsymbol{u}},\mathbf{r}^{\phi}\}$ from equation (1), where $\{\boldsymbol{u}^h,\phi^h\}$ represents the finite element approximations of the displacement and phase-field variables, respectively. For an incrementally applied load where $\mathbf{z}:=\mathbf{z}_{n-1}+\Delta\mathbf{z}$ with $n\geq 1$, the residual vector is approximated using Taylor series expansion, which when truncated to first-order terms, yields

$$\Delta\mathbf{z}=-\mathbf{K}_{n-1}^{-1}\mathbf{g}(\mathbf{z}_{n-1}), \tag{6}$$

where $\mathbf{K}$ is called tangent matrix. Due to the non-convexity of the underlying energy functional, the tangent matrix in Newton-Raphson method becomes indefinite. Herein a weak coupling is adopted, where the inter-field coupling is neglected.

Although simply employing weak coupling is challenging due to the strong coupling with the phase-field [9] and lack of convexity, it can be alleviated by solving one field at a time. In fact, Bourdin et al. [6] show that each field in the functional (1) is convex if the other field is fixed. Based on this statement, the alternating minimization solver (AM), also known as staggered solver, is a two-step iterative method where each field is solved sequentially until convergence is achieved for both $\boldsymbol{u}^h$ and ϕ^h. The algorithm is detailed in Ramos et al. [19].

3.1 Limited-memory Broyden-Fletcher-Goldfarb-Shanno solver (L-BFGS)

Quasi-Newton methods have been widely used in a variety of optimization problems due to their computational economy and efficiency. While Newton's method requires $\mathcal{O}(\mathrm{dim}^2)$ computational effort per iteration to construct and factorize the tangent matrix, quasi-Newton methods approximate curvature information through consecutive gradient differences, demanding only $\mathcal{O}(\mathrm{dim})$ operations, where dim represents the size of $\mathbf{z}$. The fundamental approach involves updating the solution as $\mathbf{z}_{k+1}:=\mathbf{z}_k+\lambda_k\Delta\mathbf{z}_k$, where λ_k is the step size along the descent direction $\Delta\mathbf{z}_k$, and establishing the secant condition $\tilde{\mathbf{K}}_{k+1}\mathbf{s}_k=\mathbf{y}_k$, where $\mathbf{s}_k:=\mathbf{z}_{k+1}-\mathbf{z}_k$ and $\mathbf{y}_k:=\mathbf{g}_{k+1}-\mathbf{g}_k$ represent solution increments and gradient differences, respectively.

The Broyden-Fletcher-Goldfarb-Shanno (BFGS) method [20] represents the most widely used quasi-Newton approach, providing the most conservative change relative to $\tilde{\mathbf{K}}_k^{-1}$. The resulting update formula is expressed as

$$\tilde{\mathbf{K}}_{k+1}^{-1}=\left(\mathbf{I}-\rho_k\mathbf{s}_k\mathbf{y}_k^T\right)\tilde{\mathbf{K}}_k^{-1}\left(\mathbf{I}-\rho_k\mathbf{y}_k\mathbf{s}_k^T\right)+\rho_k\mathbf{s}_k\mathbf{s}_k^T, \tag{7}$$

where $\rho_k=1/\mathbf{s}_k^T\mathbf{y}_k$ denotes the curvature parameter. However, consecutive BFGS updates gradually transform the initially sparse matrix into a dense structure, resulting in quadratic memory requirements that pose challenges for large-scale problems. To address this limitation, the limited memory BFGS (L-BFGS) method [21] maintains only a history of the most recent m updates of vectors $\mathbf{s}_k$ and $\mathbf{y}_k$, preserving matrix sparsity while requiring linear memory scaling.

For non-convex optimization problems, the curvature condition $\mathbf{s}_k^T\mathbf{y}_k>0$ must be satisfied to ensure that the updated matrix $\tilde{\mathbf{K}}_{k+1}^{-1}$ inherits the positive definite property of the initial guess. A modified BFGS approach [22] handles curvature condition violations through the conditional update formula

$$\tilde{\mathbf{K}}_{k+1}^{-1}=\begin{cases}\left(\mathbf{I}-\rho_k\mathbf{s}_k\mathbf{y}_k^T\right)\tilde{\mathbf{K}}_k^{-1}\left(\mathbf{I}-\rho_k\mathbf{y}_k\mathbf{s}_k^T\right), & \text{if } \mathbf{s}_k^T\mathbf{y}_k>0\\ \tilde{\mathbf{K}}_k^{-1}, & \text{otherwise,}\end{cases} \tag{8}$$

where updates are applied only when the curvature condition is satisfied, otherwise retaining the previous approximation. This modification proves particularly beneficial during unstable crack propagation phases in phase-field models, where non-convexity becomes pronounced. The complete L-BFGS algorithm has been implemented in the open-source `BORAM` repository [23], developed in `C++` with minimal dependencies, facilitating integration with existing finite element frameworks. The full algorithm is described in Ramos et al. [19].

3.2 Quasi-Newton line search for L-BFGS

Convergence is not guaranteed by just using either the standard (7) or the modified (8) BFGS method. In fact, in tests performed in this work, both BFGS approaches diverge in load steps with unstable crack propagation. To avoid the divergence, a line search is required to control the step size along the direction $\Delta\mathbf{z}_k$ [21].

Line search methods have been employed to prevent divergence of the Newton-Raphson algorithm in phase-field analysis [7, 9, 10]. These methods typically involve evaluating the energy functional $\tilde{\mathcal{E}}$ and its directional derivative $\tilde{\mathcal{E}}_\lambda$ at multiple points along the search direction to find an optimal step size λ_k that minimizes the energy, which is computationally expensive for large-scale problems. Moreover, energy monitoring is only applicable to variationally consistent formulations, which excludes many practical phase-field models with history variables. The non-variational nature of these models becomes evident as the pseudo energy functional behavior contradicts its derivative, making traditional energy-based line search methods unsuitable.

To overcome these limitations, a gradient-based quasi-Newton line search method is proposed that circumvents energy evaluation requirements. The method seeks to minimize

$$\arg\min\{\tilde{\mathcal{E}}(\mathbf{z}_k + \lambda\Delta\mathbf{z}_k) \mid \mathbf{z}_k \in \boldsymbol{\mathcal{V}}_n \times \mathcal{D}_n,\ \Delta\mathbf{z}_k \in \boldsymbol{\mathcal{V}}_n \times \mathcal{D}_n,\ \lambda \in \mathbb{R}\}. \tag{9}$$

by finding the root of $\tilde{\mathcal{E}}_\lambda = 0$. Using Taylor series expansion and secant method approximation to avoid computing the tangent matrix at each iteration, the step length update is given by

$$\lambda_{l+1} = \lambda_l - \Delta\lambda_{l-1}\frac{\left(\mathbf{g}_l\right)^T \Delta\mathbf{z}_k}{\left(\mathbf{y}_{l-1}\right)^T \Delta\mathbf{z}_k} \tag{10}$$

The line search activates based on curvature conditions rather than energy monitoring. The activation criterion is

$$\begin{cases} \mathbf{z}_{k+1} = \mathbf{z}_k + \lambda_k\Delta\mathbf{z}_k, & \mathbf{s}_k^T\mathbf{y}_k > \texttt{TOL}_{\texttt{LS}}^{\texttt{act}} \\ \mathbf{z}_{k+1} = \mathbf{z}_k + \Delta\mathbf{z}_k, & \text{otherwise,} \end{cases} \tag{11}$$

using $\texttt{TOL}_{\texttt{LS}}^{\texttt{act}} = 10^{-5}$ and convergence tolerance $\texttt{TOL}_{\texttt{LS}} = 10^{-4}$. A detailed description of the proposed line search method is provided in Ramos et al. [19].

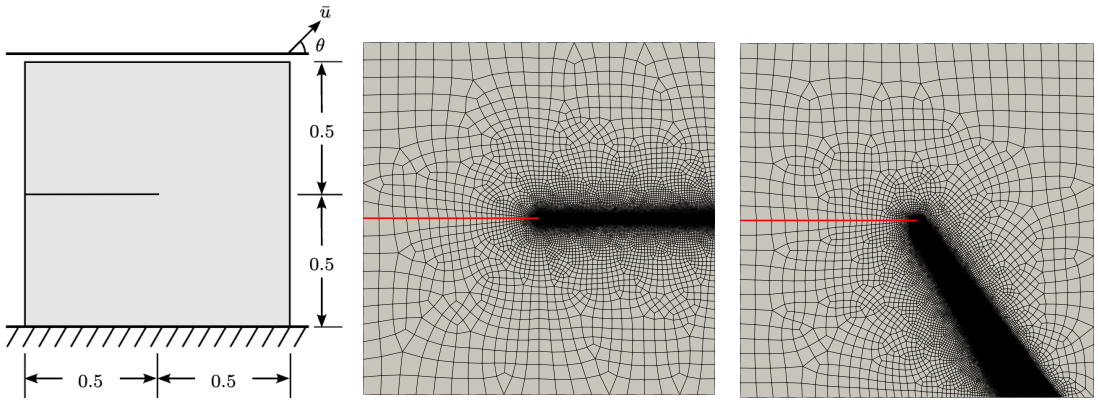
The proposed method offers several advantages over existing approaches. It operates independently of energy evaluation, requiring only gradient information, which makes it computationally efficient with an average of 5 iterations needed to find the optimal λ_k. The method has an unrestricted domain, allowing λ_k to exceed unity for potential convergence acceleration, and can capture negative step sizes when beneficial. Numerical experiments demonstrate that the method maintains stability in extreme cases with high energy differences, handles optimal step sizes exceeding unity, and provides control to the L-BFGS algorithm in critical situations where standard approaches fail. Most importantly, it successfully manages the non-variational nature of phase-field models by minimizing $|\tilde{\mathcal{E}}_\lambda|$ rather than the energy itself.

4 Analyses and discussions

As the aim of this chapter is to demonstrate the effectiveness of the proposed algorithms, two numerical representative examples with both brittle and quasi-brittle failure in either mode-I and mixed-mode are considered. To consult the parameters used to configure the algorithms and the convergence criteria applied see Ramos et al. [19]. The performance of each algorithm is evaluated using a normalized time variable $\bar{T} = T_n/T_{\text{AM}}$, which T_n represents the accumulated time required for each algorithm to reach step n, and T_{AM} represents the total time used by AM algorithm to completely simulate a given problem. Furthermore, for L-BFGS each matrix updated is counted as an iteration. It is important to emphasize that the line search procedure is required in all analyses with the L-BFGS algorithm. Without the aid of the line search, the L-BFGS algorithm diverges in all examples.

The computational domain is discretized in quadrilateral bilinear finite elements generated by Gmsh [24]. Initial cracks are modeled via geometry and mesh discretization.

As shown in Figure 1a, the problem consists of a square plate of length 1 mm with a pre-existing straight horizontal crack of length 0.5 mm located at the center of the left edge. The bottom edge is fixed, while the direction of the displacement applied to the top edge renders two problems: tension test subjected to a vertical displacement ($\theta = 90°$), and a shear test under horizontal displacement ($\theta = 0°$).



(a) (b) (c)

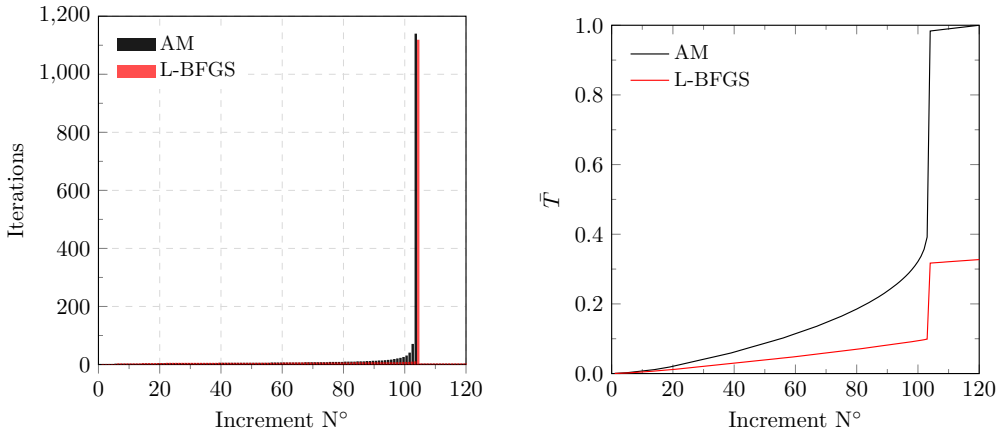
Figure 1. **Single-edge notched plate**: (a) Geometry (mm) and boundary conditions. The tensile and shear test cases are represented by $\theta = 90°$ and $\theta = 0°$, respectively. Finite element discretizations for (b) Tensile test case (22,566 elements) and (c) Shear test case (66,933 elements).

The material properties are chosen as $E = 210$ kN/mm^2, $\mathcal{G}_c = 2.7 \times 10^{-3}$ kN/mm, and $\nu = 0.3$ to match the parameters of the same example in Wu and Huang [25]. The mesh considers an *a priori* defined subdomain with a fine mesh of size $h = 0.001$ mm where the phase-field evolution is expected (see Figure 1). A length scale $\ell = 0.005$ mm and Plane stress state is adopted in all simulations.

4.1 Tensile test case

Let us first consider the tensile test case, where unstable crack growth through the specimen occurs instantaneously. In this test case, no split of the strain energy is required since the load is strictly tensile. Following Wu and Huang [25], the prescribed vertical displacement $\bar{u} = 0.06$ mm is applied in two stages: the first 0.04 mm is applied in 20 equal increments, and the remaining 0.02 mm is applied in 100 equal increments.

Figure 2a shows the number of iterations required by each algorithm to achieve convergence at each increment. Interestingly, although both the AM and L-BFGS algorithms lead to a similar number of iterations during the brutal crack propagation step, the total time required to solve the problem remains significantly lower for L-BFGS (see Figure 2b). This is explained by the fewer assembly operations of the stiffness matrix per increment for the L-BFGS. For this example, the L-BFGS is about 3 times faster than the AM algorithm.



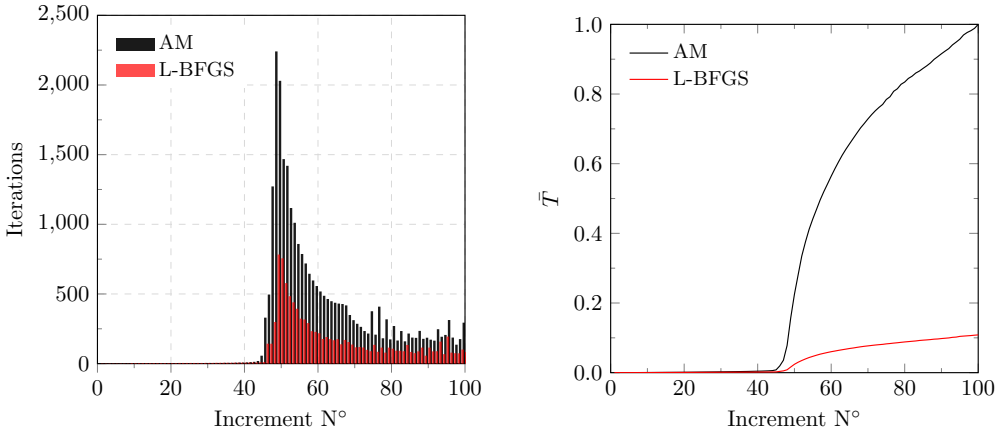
(a) (b)

Figure 2. **Single-edge notched plate under tension**: (a) Iteration number. (b) Accumulated time.

4.2 Shear test case

The same specimen is now subject to shear loading, leading to a stable crack growth where the mixed-mode tip conditions produce a damage evolution towards the lower part of the sample. In this test case, a prescribed horizontal displacement $\bar{u} = 0.02$ mm is applied in 100 equal increments, as done by [25].

The number of iterations required for convergence each algorithm to converge is rather different, as we can see in Figure 3a. In fact, the L-BFGS algorithm requires much fewer iterations compared to AM solver. Additionally, the L-BFGS algorithms achieved a significant saving in CPU time compared to AM solver, leading to a total time around 10 times smaller than the AM algorithm, as shown in Figure 3b.



(a) (b)

Figure 3. **Single-edge notched plate under shear**: (a) Iteration number. (b) Accumulated time.

5 Conclusions

This work presented a novel quasi-Newton line search strategy tailored for the Limited Broyden–Fletcher –Goldfarb–Shanno (L-BFGS) algorithm in phase-field fracture analysis. The study aimed to enhance the robustness and efficiency of monolithic solvers when dealing with highly nonlinear and non-convex energy functionals, particularly in cases involving rapid crack evolution. By incorporating a gradient-based line search, the proposed method effectively mitigates the divergence issues. Moreover, such an approach can be applied to variational and non-variational formulations since no assumptions are made regarding the energy functional, providing a versatile framework for phase-field fracture simulations. The algorithm is evaluated through multiple numerical experiments, covering brittle and quasi-brittle fracture scenarios. The results demonstrated that the proposed method significantly reduces computational cost while maintaining accuracy compared to the traditional alternating minimization approach. A stand-alone C++ implementation of the proposed method is available in the `BORAM` repository at `https://github.com/gfemuillinois/BORAM`.

Acknowledgements. Authors Caio S. Ramos and Sergio P.B. Proença would like to acknowledge the support provided by the University of São Paulo and the financial support provided by the São Paulo Research Foundation, Brazil (FAPESP) under project numbers 2019/00434-7 and 2020/14605-5. Author Nathan Shauer acknowledges the financial support provided by the São Paulo Research Foundation, Brazil (FAPESP) under project number 2024/06917-8.

Authorship statement. The authors hereby confirm that they are the sole liable persons responsible for the authorship of this work, and that all material that has been herein included as part of the present paper is either the property (and authorship) of the authors, or has the permission of the owners to be included here.

References

[1] A. A. Griffith. The phenomena of rupture and flow in solids. *Philosophical Transactions of the Royal Society of London. Series A, Containing Papers of a Mathematical or Physical Character*, vol. 221, pp. 163–198, 1921.

[2] I. Babuška and J. M. Melenk. The partition of unity finite element method. *International Journal for Numerical Methods in Engineering*, vol. 40, n. 4, pp. 727–758, 1997.
[3] T. Belytschko and T. Black. Elastic crack growth in finite elements with minimal remeshing. *International Journal for Numerical Methods in Engineering*, vol. 45, n. 5, pp. 601–620, 1999.
[4] C. A. Duarte and J. T. Oden. *H-p* clouds — an *h-p* meshless method. *Numerical Methods for Partial Differential Equations*, vol. 12, n. 6, pp. 673–705, 1996.
[5] G. Francfort and J.-J. Marigo. Revisiting brittle fracture as an energy minimization problem. *Journal of the Mechanics and Physics of Solids*, vol. 46, n. 8, pp. 1319–1342, 1998.
[6] B. Bourdin, G. Francfort, and J.-J. Marigo. Numerical experiments in revisited brittle fracture. *Journal of the Mechanics and Physics of Solids*, vol. 48, n. 4, pp. 797–826, 2000.
[7] T. Gerasimov and L. De Lorenzis. A line search assisted monolithic approach for phase-field computing of brittle fracture. *Computer Methods in Applied Mechanics and Engineering*, vol. 312, pp. 276–303. Phase Field Approaches to Fracture, 2016.
[8] T. Heister, M. F. Wheeler, and T. Wick. A primal-dual active set method and predictor-corrector mesh adaptivity for computing fracture propagation using a phase-field approach. *Computer Methods in Applied Mechanics and Engineering*, vol. 290, pp. 466–495, 2015.
[9] T. Wick. Modified newton methods for solving fully monolithic phase-field quasi-static brittle fracture propagation. *Computer Methods in Applied Mechanics and Engineering*, vol. 325, pp. 577–611, 2017.
[10] O. Lampron, D. Therriault, and M. Lévesque. An efficient and robust monolithic approach to phase-field quasi-static brittle fracture using a modified newton method. *Computer Methods in Applied Mechanics and Engineering*, vol. 386, pp. 114091, 2021.
[11] C. Miehe, F. Welschinger, and M. Hofacker. Thermodynamically consistent phase-field models of fracture: Variational principles and multi-field fe implementations. *International Journal for Numerical Methods in Engineering*, vol. 83, n. 10, pp. 1273–1311, 2010.
[12] H. Amor, J.-J. Marigo, and C. Maurini. Regularized formulation of the variational brittle fracture with unilateral contact: Numerical experiments. *Journal of the Mechanics and Physics of Solids*, vol. 57, n. 8, pp. 1209–1229, 2009.
[13] J.-Y. Wu, Y. Huang, and V. P. Nguyen. On the bfgs monolithic algorithm for the unified phase field damage theory. *Computer Methods in Applied Mechanics and Engineering*, vol. 360, pp. 112704, 2020.
[14] J.-Y. Wu, Y. Huang, H. Zhou, and V. P. Nguyen. Three-dimensional phase-field modeling of mode i + ii/iii failure in solids. *Computer Methods in Applied Mechanics and Engineering*, vol. 373, pp. 113537, 2021.
[15] Y. Yu, C. Hou, T. Rabczuk, and M. Zhao. An adaptive incremental solution scheme for the phase field model of fracture. *Engineering Fracture Mechanics*, vol. 315, pp. 110799, 2025.
[16] L. Ambrosio and V. M. Tortorelli. Approximation of functional depending on jumps by elliptic functional via t-convergence. *Communications on Pure and Applied Mathematics*, vol. 43, n. 8, pp. 999–1036, 1990.
[17] J.-Y. Wu. A unified phase-field theory for the mechanics of damage and quasi-brittle failure. *Journal of the Mechanics and Physics of Solids*, vol. 103, pp. 72–99, 2017.
[18] M. Ambati, T. Gerasimov, and L. De Lorenzis. A review on phase-field models of brittle fracture and a new fast hybrid formulation. *Computational Mechanics*, vol. 55, n. 2, pp. 383–405, 2015.
[19] C. S. Ramos, C. A. Duarte, N. Shauer, and S. P. Proença. Phase-field fracture analysis: A gradient-based line search strategy for the l-bfgs algorithm. *Computer Methods in Applied Mechanics and Engineering*, vol. 445, pp. 118170, 2025.
[20] C. G. Broyden. The convergence of a class of double-rank minimization algorithms 1. general considerations. *IMA Journal of Applied Mathematics*, vol. 6, n. 1, pp. 76–90, 1970.
[21] H. Matthies and G. Strang. The solution of nonlinear finite element equations. *International Journal for Numerical Methods in Engineering*, vol. 14, n. 11, pp. 1613–1626, 1979.
[22] D.-H. Li and M. Fukushima. On the global convergence of the bfgs method for nonconvex unconstrained optimization problems. *SIAM Journal on Optimization*, vol. 11, n. 4, pp. 1054–1064, 2001.
[23] C. S. Ramos and N. Shauer. L-bfgs for phase-field fracture. `https://github.com/gfemuillinois/BORAM`, 2025.
[24] C. Geuzaine and J.-F. Remacle. Gmsh: A 3-d finite element mesh generator with built-in pre- and post-processing facilities. *International Journal for Numerical Methods in Engineering*, vol. 79, n. 11, pp. 1309–1331, 2009.
[25] J.-Y. Wu and Y. Huang. Comprehensive implementations of phase-field damage models in abaqus. *Theoretical and Applied Fracture Mechanics*, vol. 106, pp. 102440, 2020.